*Proceeding Paper*

# Analysis of Subglacial Lake Activity in Recovery Ice Stream with ICESat-2 Laser Altimetry †

**Yangyang Chen** [1,2]

1 College of Surveying and Geo-Informatics, Tongji University, Shanghai 200092, China; 2133678@tongji.edu.cn
2 Center for Spatial Information Science and Sustainable Development Applications, Tongji University, Shanghai 200092, China
† Presented at the 5th International Electronic Conference on Remote Sensing, 7–21 November 2023; Available online: https://ecrs2023.sciforum.net/.

**Abstract:** The latest laser altimetry technology employed by NASA's Ice, Cloud, and Land Elevation Satellite-2 (ICESat-2) enables the capture of denser and more precise spatial details. Here, we utilize ICESat-2 data from September 2018 to July 2022 to replicate and analyze the dynamics of the recovery ice stream's subglacial lake system. To investigate the pathways of subglacial water transfer and determine the outline of subglacial lakes, we employ the differential digital elevation model (DEM) method to depict the surface elevation changes of each subglacial lake at monthly intervals. Our findings indicate significant migration in the activity location of 4 lakes. Notably, Rec1, previously regarded as a single lake, performed as two distinct lakes during the study. Furthermore, we identify two large-scale lakes with subglacial water flux reaching 0.5 $km^3$.

**Keywords:** Recovery Ice Stream (RIS); ICESat-2; active subglacial lakes

## 1. Introduction

The Recovery Ice Stream (RIS) is one of the longest ice streams in Antarctica [1], annually discharging a significant mass of ice into the Southern Ocean [2]. Beneath the RIS are numerous active subglacial lakes whose drainage and storage directly impact the flow velocity of the entire ice stream [3,4]. This, in turn, has a considerable influence on ice dynamics, grounding line stability, and the mass balance of the East Antarctic Ice Sheet [4]. Previous research based on surface structure characteristics and radio-echo sounding (RES), also known as ice-penetrating radar, has revealed a significant number of subglacial lakes in RIS upstream [5]. These lakes are closely associated with the development and rapid movement of the RIS. Ever since scientists discovered that surface deformation resulting from subglacial lake activity leads to anomalously large features [6], numerous active lakes within the RIS basin have also been captured by ICESat data [7,8]. Smith et al. confirmed the positions of 11 active lakes beneath the RIS by calculating elevation changes using 4.5 years of ICESat data [3]. However, due to the sparse nature of the ICESat track, accurately determining the lake surface area and estimating changes in subglacial water volume proved challenging [3]. After the retirement of ICESat in 2009, the 11-year Ice-Bridge campaign conducted multiple investigations in the RIS basin, providing years of airborne altimetry data and ice radar data [9]. Fricker et al. were the first to combine ICE-Sat data, IceBridge datasets, and MODIS imagery, extending the monitoring record of subglacial lakes within the RIS until 2012, revealing the activity of the RIS's subglacial lake system [10].

In this study, we utilized all the ICESat-2 data from September 2018 to August 2022 to quantitatively measure the elevation changes of the known active subglacial lakes corresponding to the ice surface in the RIS. This allowed us to assess the accuracy of past

subglacial lake outlines and quantitatively estimate the magnitude of water filling and drainage during each subglacial lake activity. Furthermore, we conducted a comprehensive analysis of the hydrological connections among subglacial lakes within the Recovery Glacier basin. We successfully monitored active subglacial lakes on a time scale shorter than the repeat cycle of ICESat-2, capturing subglacial lake activity with higher precision, detail, and speed compared to previous studies.
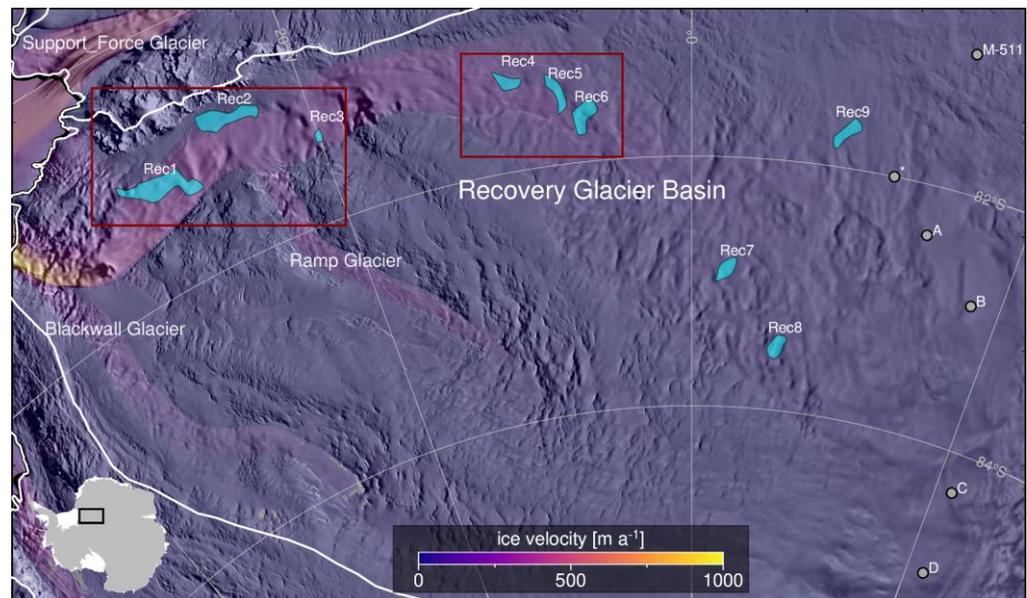


**Figure 1.** Map of subglacial lakes of RIS and study area. Cyan polygons indicate hypothesized locations of active subglacial lakes [11], and gray-filled circles represent stable subglacial lakes [12]. The white bold line corresponds to the boundary of the Antarctic drainage basin [13], and the black bold line represents the grounding line [14]. The area within the dark red box in Figure 2 is highlighted, with the underlying map depicting the overlaid ice flow velocity from MOA [15–17]. The inset in the bottom left corner shows the location of Figure 1 [18].
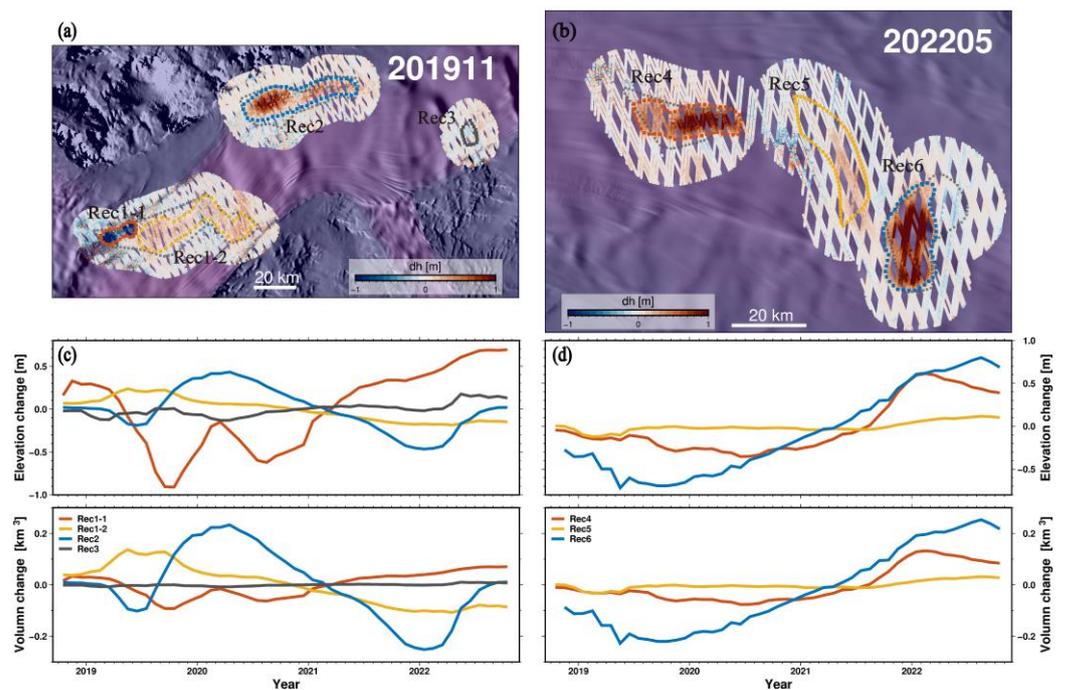


**Figure 2.** Spatial and temporal changes of the subglacial lakes in the RIS. Maps of subglacial lake surface-height anomalies for (**a**) RIS downstream during October 2019–December 2019 and (**b**) RIS

upstream during April 2022–June 2022, with the derived subglacial lake time series for (**c**) Rec1-1, Rec1-2, Rec2, Rec3, and (**d**) Rec4, Rec5, and Rec6. The derived new lake outline colors in (**a**,**b**) correspond to the time series in (**c**,**d**). The lake outlines of Siegfried et al. appear as black blocks with 70% transparency. The white arrows indicate the direction of the RIS.

## 2. Area and Data

Our study area encompasses the drainage basin of the RIS, located in the Queen Maud Land region of Eastern Antarctica. It spans an approximate area of 996,000 square kilometers, accounting for around 8% of the total area of Southeast Antarctica [19]. In the inventory of active subglacial lakes published in 2018, 9 of them were from the RIS[11]. They constituted the initial lake outlines utilized in our study. In addition to the active subglacial lakes, six non-active lakes have been identified upstream of the RIS through radar or seismic surveys [12]. In this study, we selected the six subglacial lakes situated along the trunk of the RIS as our interest area.

The ICESat-2 data covers all known active subglacial lakes [20]. We conducted experimental analysis on selected active subglacial lakes of the RIS based on the level 3a ATL06 data (Land Ice Height), v005 [21,22]. The ATL06 data provides average heights along the orbit direction, with a 40-m segment used for averaging and a 20-m along-track resolution. Considering the precision and spatial distribution characteristics of ATL06 datasets, we have devised an improved approach, according to Siegfried et al. [20], to maximize the advantages of the ICESat-2 data and reconstruct the activity of subglacial lakes within the RIS.

## 3. Methods

### 3.1. Lake Activity from ICESat-2 ATL06 Measurements

We downloaded complete ICESat-2 data from September 2018 to August 2022 for subglacial lake detection. Firstly, we applied a basic initial filtering scheme on the ATL06 product, using the overall quality summary flag to remove low-quality data. The remaining dataset was then used to generate a reference Digital Elevation Model (DEM) in the GMT [18] software. The height anomaly was calculated as the difference between the actual measured elevation value and the interpolated elevation value from the reference DEM. To reduce the data input of ICESat-2, we employed a buffer zone of 10 km beyond the initial lake contours provided by Siegfried et al. [11] as the graphical input for each lake. Within each lake region, we computed and collected the surface height anomaly at monthly intervals. These surface height anomalies were subsequently plotted to dynamically illustrate the drainage and accumulation patterns of each lake, as shown in Figure 2a,b.

### 3.2. Time Series Elevation and Volume Changes

The monthly height anomaly maps indicate a remarkable migration of the lake outlines compared to the inventory provided by Siegfried et al. [11]. In order to better estimate the water flux associated with the lake activities during each lake fill-drain cycle, we updated the existing lake outlines. By rolling averaging the height anomalies within the new lake outlines on a 90-day period and step by 30-day, we generated a surface height anomaly time series. Also, the height anomaly time series of the stable ice sheet was derived from estimating the elevation within a 10-km-wide annular region surrounding each lake. To exclude interference from the elevation changes caused by ice flow velocity etc. factors, the static ice sheet's height anomaly time series was subtracted. The volume change was calculated by multiplying the height anomaly by the lake area determined by the lake outlines. To quantify the interpolation accuracy in differential DEM, we employed a Monte Carlo approach. Initially, we excluded data from one orbit within the lake region and used the remaining orbit data to synthesize a DEM. The difference between the synthesized DEM and the actual measurements from the excluded orbit was then computed

and statistically analyzed. This process was repeated iteratively by removing one orbit at a time until the calculations were completed. Since the calculated elevation change errors were smaller than the line width of the curves in Figure 2c,d, they are not shown here.

## 4. Results & Discussion

We discuss the elevation change and volume change of the 6 lakes, starting at the most upstream lake and moving down-RIS. Rec6 (316 km²) has experienced an area reduction of nearly one-fifth. By examining MovieS2, we observe that the elevation trends in the northeast corner of the original Rec6 are opposite to its main body, indicating an exchange of subglacial water between Rec6 and its northeastern corner region. From late 2018 to early 2019, Rec6 underwent a period of drainage, resulting in a decrease in elevation of approximately 0.5 m. Subsequently, a prolonged period of water accumulation ensued, lasting until the end of the observation period. The maximum elevation changes in the center of Rec6 reached 4.5 m, corresponding to the filling of nearly 0.5 km³ of subglacial water. Downstream of Rec6 are two smaller lakes, Rec4 (217 km²) and Rec5 (273 km²). While Rec5 experienced minimal spatial repositioning, Rec4 exhibited noticeable outline migration. The subtle elevation variations in Rec5 align closely with the activity of Rec6. For instance, during Rec6's extended period of water accumulation, Rec5's surface elevation exhibited a slight uplift, indicating the overflow of subglacial water from Rec6 to Rec5. Comparing the elevation change time series of Rec4 and Rec6, it is evident that approximately seven months after Rec6 began its water accumulation, Rec4 followed suit. This suggests that after undergoing rapid drainage, Rec6 remained at a lower water level until it reached a certain threshold before initiating downstream water release. Towards the end of the observation period, Rec4 gradually started its discharge in February 2022, whereas Rec6's discharge occurred in August 2022. We speculate that this is due to Rec4 continuously releasing water to a lower water level, resulting in a sufficient hydraulic head difference between Rec6 and Rec4, thus triggering the opening of Rec6's floodgates for water release.

The other 4 lakes are situated downstream of the RIS. Rec3 (58 km²) exhibited minimal changes throughout the entire ICESat-2 observation period. Rec2 (539 km²), located adjacent to the Shackleton Range, underwent two connected fill-drain cycles. The second drainage period lasted from February 2020 until January 2022, spanning almost two years, resulting in 1 m surface deflation. Rec1, previously believed to be a single lake, was identified as two distinct lakes based on surface height anomaly maps and time series of elevation changes. After a surface uplift of 0.2 m between November 2018 and April 2019, Rec1-2 (579 km²) experienced a gradual subsidence of 0.4 m from October 2019 to August 2022. Rec1-1 (101 km²) underwent a surface subsidence of 1.3 m from October 2018 to October 2019, followed by a rapid backfilling of approximately 0.8 m over the next five months. After a short discharge, the surface elevation of Rec1-1 continued to increase by 1.4 m. Regarding the surface elevation changes of Rec1-1, Rec1-2, and Rec2 from 2019 to 2021, we propose the following hypothesis: Firstly, downstream Rec1-2 discharged water into Rec1-1, coinciding with Rec2 receiving subglacial water from the upstream. This likely resulted in a hydraulic head difference, allowing the breakthrough of hydraulic barriers and the continued transport of subglacial water towards Rec1-2. In the study by Siegfried et al. [10], it was mentioned that Rec1 had two outlets for subglacial water, one towards the north, through the Shackleton Range, and another towards the southwest, parallel with RIS. We speculate that the subglacial water rapidly opened the southwest pathway of Rec1, releasing subglacial water, and then swiftly closed in July 2020. Consequently, all subglacial water from Rec2 and Rec1-2 entered Rec1-1. Furthermore, the surface uplift of Rec2 in 2022 appears to correspond to the surface deflation of Rec4. Simultaneously, the rate of water filling in Rec1-1 decreased accordingly.

*Environ. Sci. Proc.* **2023**, *27*, x FOR PEER REVIEW

5 of 6

## 5. Conclusions

We have demonstrated the capability of ICESat-2 laser altimetry technology to acquire unprecedented spatial and temporal details of surface elevation changes in active subglacial lakes. By depicting dynamic patterns of surface elevation changes, we investigate the hydrological processes beneath the RIS. The RIS exhibits typical characteristics of a terrestrial river, being surrounded by mountain ranges and lying on a bedrock trough that exceeds 2 km in depth. The 6 active lakes under the primary trunk of the RIS are interconnected hydrologically. Based on our observations of subglacial lake activity, we have identified that the original Rec1 actually consists of two separate subglacial lakes. We have also found that the extent of the two more active lakes, Rec2 and Rec6, has decreased in size compared to their previously reported positions. Rec4, located downstream of Rec6, has undergone significant positional displacement. While we have drawn upon existing literature that suggests the presence of two bifurcated outlets for Rec1, our experimental results provide only tentative explanations and lack direct evidence support, indicating an avenue for future research.

**Supplementary Materials:** The following supporting information can be downloaded at: www.mdpi.com/xxx/s1, Video S1 and Video S2, are respectively the monthly calculated surface-height anomalies derived from ICESat-2 over three-month periods. Video S1 covers the downstream lakes of the RIS, while Video S2 covers the upstream lakes of the RIS.

**Funding:**

**Institutional Review Board Statement:**

**Informed Consent Statement:**

**Data Availability Statement:** The ICESat-2 ATL06 data used in this manuscript are freely available from the National Snow and Ice Data Center (https://nsidc.org/data/data-access-tool/ATL06/versions/5). The data of the active subglacial lake and the stable subglacial lake were obtained respectively from Siegfried et al. (https://doi.org/10.5281/zenodo) and Livingstone et al. (https://doi.org/10.1038/s43017-021-00246-9).

**Conflicts of Interest:**

## References

1. Langley, K.; Tinto, K.; Block, A.; Bell, R.; Kohler, J.; Scambos, T. Onset of Fast Ice Flow in Recovery Ice Stream, East Antarctica: A Comparison of Potential Causes. *J. Glaciol.* **2014**, *60*, 1007–1014. https://doi.org/10.3189/2014JoG14J067.
2. Langley, K.; Kohler, J.; Matsuoka, K.; Sinisalo, A.; Scambos, T.; Neumann, T.; Muto, A.; Winther, J.-G.; Albert, M. Recovery Lakes, East Antarctica: Radar Assessment of Sub-Glacial Water Extent: RECOVERY LAKES, EAST ANTARCTICA. *Geophys. Res. Lett.* **2011**, *38*. https://doi.org/10.1029/2010GL046094.
3. Smith, B.E.; Fricker, H.A.; Joughin, I.R.; Tulaczyk, S. An Inventory of Active Subglacial Lakes in Antarctica Detected by ICESat (2003–2008). *J. Glaciol.* **2009**, *55*, 573–595. https://doi.org/10.3189/002214309789470879.
4. Dow, C.F.; Werder, M.A.; Babonis, G.; Nowicki, S.; Walker, R.T.; Csatho, B.; Morlighem, M. Dynamics of Active Subglacial Lakes in Recovery Ice Stream. *JGR Earth Surface* **2018**, *123*, 837–850. https://doi.org/10.1002/2017JF004409.
5. Bell, R.E.; Studinger, M.; Shuman, C.A.; Fahnestock, M.A.; Joughin, I. Large Subglacial Lakes in East Antarctica at the Onset of Fast-Flowing Ice Streams. *Nature* **2007**, *445*, 904–907. https://doi.org/10.1038/nature05554.
6. Fricker, H.A.; Padman, L. Ice Shelf Grounding Zone Structure from ICESat Laser Altimetry. *Geophys. Res. Lett.* **2006**, *33*, L15502. https://doi.org/10.1029/2006GL026907.
7. Fricker, H.A.; Scambos, T. Connected Subglacial Lake Activity on Lower Mercer and Whillans Ice Streams, West Antarctica, 2003–2008. *J. Glaciol.* **2009**, *55*, 303–315. https://doi.org/10.3189/002214309788608813.
8. Fricker, H.A.; Scambos, T.; Bindschadler, R.; Padman, L. An Active Subglacial Water System in West Antarctica Mapped from Space. *Science* **2007**, *315*, 1544–1548. https://doi.org/10.1126/science.1136897.
9. Diez, A.; Matsuoka, K.; Ferraccioli, F.; Jordan, T.A.; Corr, H.F.; Kohler, J.; Olesen, A.V.; Forsberg, R. Basal Settings Control Fast Ice Flow in the Recovery/Slessor/Bailey Region, East Antarctica. *Geophys. Res. Lett.* **2018**, *45*, 2706–2715. https://doi.org/10.1002/2017GL076601.
10. Fricker, H.A.; Carter, S.P.; Bell, R.E.; Scambos, T. Active Lakes of Recovery Ice Stream, East Antarctica: A Bedrock-Controlled Subglacial Hydrological System. *J. Glaciol.* **2014**, *60*, 1015–1030. https://doi.org/10.3189/2014JoG14J063.
11. Siegfried, M.R.; Fricker, H.A. Thirteen Years of Subglacial Lake Activity in Antarctica from Multi-Mission Satellite Altimetry. *Ann. Glaciol.* **2018**, *59*, 42–55. https://doi.org/10.1017/aog.2017.36.

12. Livingstone, S.J.; Li, Y.; Rutishauser, A.; Sanderson, R.J.; Winter, K.; Mikucki, J.A.; Björnsson, H.; Bowling, J.S.; Chu, W.; Dow, C.F.; et al. Subglacial Lakes and Their Changing Role in a Warming Climate. *Nat. Rev. Earth Environ.* **2022**, *3*, 106–124. https://doi.org/10.1038/s43017-021-00246-9.

13. Mouginot, J.; Scheuchl, B.; Rignot, E. *MEaSUREs Antarctic Boundaries for IPY 2007–2009 from Satellite Radar, Version 2*; NASA National Snow and Ice Data Center Distributed Active Archive Center: Boulder, Colorado USA, 2017.

14. Depoorter, M.A.; Bamber, J.L.; Griggs, J.A.; Lenaerts, J.T.M.; Ligtenberg, S.R.M.; Van Den Broeke, M.R.; Moholdt, G. Calving Fluxes and Basal Melt Rates of Antarctic Ice Shelves. *Nature* **2013**, *502*, 89–92. https://doi.org/10.1038/nature12567.

15. Scambos, T.A.; Haran, T.M.; Fahnestock, M.A.; Painter, T.H.; Bohlander, J. MODIS-Based Mosaic of Antarctica (MOA) Data Sets: Continent-Wide Surface Morphology and Snow Grain Size. *Remote Sens. Environ.* **2007**, *111*, 242–257. https://doi.org/10.1016/j.rse.2006.12.020.

16. Haran, T.; Bohlander, J.; Scambos, T.; Painter, T.; Fahnestock, M. *MODIS Mosaic of Antarctica 2008–2009 (MOA2009) Image Map, Version 2*; NASA National Snow and Ice Data Center Distributed Active Archive Center: Boulder, Colorado USA, 2021.

17. Mouginot, J.; Rignot, E.; Scheuchl, B. Continent-Wide, Interferometric SAR Phase, Mapping of Antarctic Ice Velocity. *Geophys. Res. Lett.* **2019**, *46*, 9710–9718. https://doi.org/10.1029/2019GL083826.

18. Wessel, P.; Luis, J.F.; Uieda, L.; Scharroo, R.; Wobbe, F.; Smith, W.H.F.; Tian, D. The Generic Mapping Tools Version 6. *Geochem. Geophys. Geosyst.* **2019**, *20*, 5556–5564. https://doi.org/10.1029/2019GC008515.

19. Rignot, E.; Bamber, J.L.; Van Den Broeke, M.R.; Davis, C.; Li, Y.; Van De Berg, W.J.; Van Meijgaard, E. Recent Antarctic Ice Mass Loss from Radar Interferometry and Regional Climate Modelling. *Nat. Geosci.* **2008**, *1*, 106–110. https://doi.org/10.1038/ngeo102.

20. Siegfried, M.R.; Fricker, H.A. Illuminating Active Subglacial Lake Processes With ICESat-2 Laser Altimetry. *Geophys. Res. Lett.* **2021**, *48*, e2020GL091089. https://doi.org/10.1029/2020GL091089.

21. Smith, B.; Fricker, H.A.; Holschuh, N.; Gardner, A.S.; Adusumilli, S.; Brunt, K.M.; Csatho, B.; Harbeck, K.; Huth, A.; Neumann, T.; et al. Land Ice Height-Retrieval Algorithm for NASA's ICESat-2 Photon-Counting Laser Altimeter. *Remote Sens. Environ.* **2019**, *233*, 111352. https://doi.org/10.1016/j.rse.2019.111352.

22. Smith, B.S.; Adusumilli, B.M.; Csathó, D.; Felikson, H.A.; Fricker, A.; Gardner, N.; Holschuh, J.; Lee, J.; Nilsson, F.S.; Paolo, M.R. et al. *ATLAS/ICESat-2 L3A Land Ice Height, Version 6*; NASA National Snow and Ice Data Center Distributed Active Archive Center: Boulder, Colorado USA, 2023.